The Plant Cell, Vol. 18, 626–638, March 2006, www.plantcell.org © 2006 American Society of Plant Biologists

The *Arabidopsis* SOMATIC EMBRYOGENESIS RECEPTOR-LIKE KINASE1 Protein Complex Includes BRASSINOSTEROID-INSENSITIVE1 [W]

Rumyana Karlova,[a,b] Sjef Boeren,[a] Eugenia Russinova,[a] José Aker,[a] Jacques Vervoort,[a] and Sacco de Vries[a,1]

[a] Laboratory of Biochemistry, Wageningen University, 6703 HA Wageningen, The Netherlands
[b] Center for BioSystems Genomics, 6700 AB Wageningen, The Netherlands

***Arabidopsis thaliana* SOMATIC EMBRYOGENESIS RECEPTOR-LIKE KINASE1 (SERK1) is a leucine-rich repeat receptor-like kinase (LRR-RLK) involved in the acquisition of embryogenic competence and in male sporogenesis. To determine the composition of the SERK1 signaling complex in vivo, we generated plants expressing the SERK1 protein fused to cyan fluorescent protein under SERK1 promoter control. The membrane receptor complex was immunoprecipitated from seedlings, and the coimmunoprecipitating proteins were identified using liquid chromatography/matrix-assisted laser desorption ionization–time of flight/mass spectrometry of the trypsin-released peptides. This approach identified two other LRR-RLKs, the BRASSINOSTEROID-INSENSITIVE1 (BRI1) receptor and its coreceptor, the SERK3 or BRI1-ASSOCIATED KINASE1 protein. In addition, KINASE-ASSOCIATED PROTEIN PHOSPHATASE, CDC48A, and 14-3-3ν were found. Finally, the MADS box transcription factor AGAMOUS-LIKE15 and an uncharacterized zinc finger protein, a member of the CONSTANS family, were identified as part of the SERK1 complex. Using blue native gel electrophoresis, we show that SERK1 and SERK3 are part of BRI1-containing multiple protein complexes with relative masses between 300 and 500 kD. The SERK1 mutant allele *serk1-1* enhances the phenotype of the weak BRI1 allele *bri1-119*. Collectively, these results suggest that apart from SERK3, SERK1 is also involved in the brassinolide signaling pathway.**

INTRODUCTION

Membrane-located leucine-rich repeat receptor-like kinases (LRR-RLKs) play important roles in plant signaling pathways. For example, the *Arabidopsis thaliana* CLAVATA1 (CLV1), BRASSINOSTEROID-INSENSITIVE1 (BRI1), ERECTA, rice (*Oryza sativa*) Xa21, HAESA-RLK5, and FLS2 genes were shown to function in shoot meristem maintenance, hormone perception, organ elongation, disease resistance, abscission, and flagellin signaling, respectively (reviewed in Torii, 2004). Extensive genetic and biochemical studies have been undertaken to identify additional components of different signaling pathways. For example, negative and positive regulators of brassinosteroid (BR) signaling were identified as the GSK-3/Shaggy-like kinase called BRASSINOSTEROID-INSENSITIVE2 (BIN2) (Li and Nam, 2002) and the nucleus-localized Ser/Thr phosphatase *bri1* Suppressor1 family (Mora-Garcia et al., 2004), respectively. Their potential substrates are the nuclear proteins BRASSINAZOLE-RESISTANT1 (BZR1) (Wang et al., 2002b) and *bri1*-EMS-SUPPRESSOR1 (BES1) (Yin et al., 2002).

[1] To whom correspondence should be addressed. E-mail sacco.devries@wur.nl; fax 31-317-484801.
The author responsible for distribution of materials integral to the findings presented in this article in accordance with the policy described in the Instructions for Authors (www.plantcell.org) is: Sacco de Vries (sacco.devries@wur.nl).
[W] Online version contains Web-only data.
Article, publication date, and citation information can be found at www.plantcell.org/cgi/doi/10.1105/tpc.105.039412.

We previously identified *Arabidopsis* SOMATIC EMBRYOGENESIS RECEPTOR-LIKE KINASE1 (SERK1), an LRR-RLK that marks the formation of embryogenic cells in culture and is expressed in ovule primordia and in both male and female gametophytes. In sporophytic tissues, SERK1 has a complex expression pattern, with expression being highest in the vascular tissue of all organs (Hecht et al., 2001; Albrecht et al., 2005; Kwaaitaal et al., 2005). Ectopic expression of *SERK1* does not result in an obvious phenotype in *Arabidopsis* plants but increases somatic embryo formation in culture (Hecht et al., 2001). SERK1 is a member of a small family of five related RLKs, all of which have five LRRs and a typical Ser-Pro–rich juxtamembrane region (Hecht et al., 2001). The SERK1 knockout alleles *serk1-1* and *serk1-2* did not have a morphological phenotype but in combination with a *serk2* null mutant resulted in complete male-sterile plants (Albrecht et al., 2005; Colcombet et al., 2005). SERK3 or BRI1-ASSOCIATED RECEPTOR KINASE1 (BAK1) is part of the BR receptor complex and is proposed to function as a coreceptor of the BRI1 protein (Li et al., 2002; Nam and Li, 2002). Recently, we showed that in living plant cells BRI1 and SERK3 interaction occurred in restricted areas of the membrane and recycled upon internalization by endocytosis (Russinova et al., 2004).

SERK1 was shown to interact with the KINASE-ASSOCIATED PROTEIN PHOSPHATASE (KAPP) that is postulated to play a role in receptor internalization (Shah et al., 2002). Using a yeast two-hybrid screen, two additional SERK1-interacting proteins, CDC48A and 14-3-3λ, were found (Rienties et al., 2005). These interactions suggested analogy with the mammalian CDC48

homologue p97/VCP complex, in which p97/VCP can be phosphorylated by the JAK-2 kinase and dephosphorylated by the phosphatase PTPH1 that associates with a 14-3-3 protein (Zhang et al., 1997, 1999). KAPP has also been reported to interact with other LRR-RLKs such as HAESA, WALL-ASSOCIATED KINASE1, FLS2, and CLV1 (reviewed in Becraft, 2002). Transgenic studies indicate that KAPP functions as a negative regulator of CLV1 and FLS2 signaling (Williams et al., 1997; Stone et al., 1998; Gomez-Gomez et al., 2001).

Identification of proteins can now be performed at high sensitivity by specific proteolytic digestion and determination of the peptide masses by mass spectrometry. This technique has been used for a systematic study of multiprotein complexes. For the epidermal growth factor receptor, a human receptor Tyr kinase, immunoprecipitation combined with matrix-assisted laser desorption ionization–time of flight/mass spectrometry (MALDI-TOF/MS) was used to identify components of the epidermal growth factor receptor signaling complex (Pandey et al., 2000). For only a few plant RLKs, the signaling complex has been defined. One example is the 105-kD CLV1 receptor that is found in two distinct protein complexes of 450 and 185 kD. The larger 450-kD complex requires functional CLV1 and CLV3 proteins for assembly and includes KAPP and a Rho GTPase-related protein (Trotochaud et al., 1999).

In this study, we have determined the composition of the SERK1 complex(es) in vivo. We combined immunoprecipitation of cyan fluorescent protein (CFP)–tagged SERK1 with rapid liquid chromatography (LC)/MALDI-TOF/MS–based protein identification. Using this method, we confirmed the presence in the SERK1 signaling complex of CDC48A (Rienties et al., 2005) and KAPP (Shah et al., 2002). Additional proteins were also found, such as another member of the 14-3-3 family, 14-3-3ν, SERK3 (BAK1) and BRI1, the MADS box transcription factor AGAMOUS-LIKE15 (AGL15), and an uncharacterized zinc finger protein. In particular, the interaction between SERK1 and BRI1 was confirmed by a genetic experiment and fluorescence lifetime imaging microscopy (FLIM) to determine Förster resonance energy transfer (FRET) between fluorescently tagged receptors. Our data show that the method used here can distinguish between individual isoforms of related members of the same protein family, confirming and extending previous screens performed using the more commonly applied yeast two-hybrid method to find interacting partners.

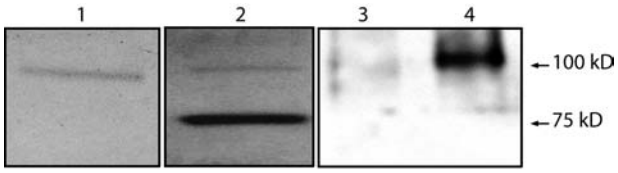

Figure 1. Detection of SERK1 and SERK1-CFP from Wild-Type and Transgenic Plants.

Total protein extracts from SERK1-CFP–transformed seedlings and wild-type seedlings were immunoprecipitated with anti-GFP antibodies. Thirty micrograms of total protein extracted from SERK1-CFP seedlings (lanes 1 and 2) and the immunoprecipitation products from SERK1-CFP seedlings (lane 4) and wild-type seedlings (lane 3) were separated on a 10% SDS-PAGE gel. The blots were incubated with anti-GFP antibodies (lanes 1, 3, and 4) or with anti–GST-SERK1 kinase antibodies (lane 2). The sizes of the marker proteins are indicated by arrows.

RESULTS

Immunoprecipitation and Detection of SERK1-CFP Protein

To purify and detect the SERK1 protein and its interacting partners directly from seedlings, C-terminal SERK1-CFP fusion proteins were stably expressed in *Arabidopsis* wild-type plants under the control of the SERK1 promoter as described (Kwaaitaal et al., 2005). The expression pattern of SERK1-CFP was identical to that of a previously characterized SERK1–yellow fluorescent protein (YFP) fusion protein (Kwaaitaal et al., 2005). Similar to SERK1-YFP–expressing plants, no unusual phenotype was observed, whereas introduction of the same SERK1 promoter-SERK1-CFP construct used here in the SERK1 knockout mutant background restored the male sterility phenotype of the double *serk1-1 serk2-2* mutant (Albrecht et al., 2005). This finding confirms that the fusion protein did not interfere with its endogenous counterpart and was fully functional. Total proteins extracted from 7-d-old SERK1-CFP–expressing seedlings were separated by SDS-PAGE, and after blotting on a membrane, the fusion proteins were detected with anti–green fluorescent protein (GFP) antibody (Figure 1, lane 1). The same protein extract was detected with anti-GST-SERK1 kinase antibodies, which recognize endogenous SERK1 as well as the SERK1-CFP fusion proteins, confirming the specificity of the anti-GFP antibodies (Figure 1, lane 2). After immunoprecipitation, an aliquot was analyzed with anti-GFP antibody to confirm that SERK1-CFP was indeed recovered in the immunoprecipitation. A band of 100 kD was recognized only in protein extracts of the transgenic line (Figure 1, lane 4) and not in extracts of wild-type seedlings (Figure 1, lane 3).

LC/MALDI-TOF/MS Identification of SERK1 and Its Interacting Partners in Vivo

To identify proteins that bind to SERK1 as extracted from SERK1-CFP–expressing seedlings, we subjected the immunoprecipitated proteins (bound to the protein A–Sepharose beads) to trypsin digestion. To reduce the influence of ion-suppression effects in MALDI-TOF/MS measurements and obtain more peptide peaks, separation of the tryptic peptides by reverse-phase column chromatography was performed before subjection to MALDI-TOF/MS measurements. As a negative control, samples obtained from an immunoprecipitated protein extract from wild-type seedlings with anti-GFP antibody were analyzed in the same way by LC/MALDI-TOF/MS.

A representative LC/MALDI-TOF/MS spectrum, recorded for fraction 9 from the 24 LC fractions obtained after trypsin digestion of the immunoprecipitated SERK1 complex, is shown in Figure 2A. In Figure 2B, a spectrum recorded for fraction 9 of the trypsin-digested immunoprecipitated negative control extract is shown. All mass-to-charge ratio (m/z) values also present in the negative control (i.e., values belonging to protein A, GFP antibodies, and proteins aspecifically immunoprecipitated by the

GFP antibodies) were removed from the *m/z* list. The remaining values were then compared with the predicted tryptic peptide masses for the *Arabidopsis* proteome as described in Methods. The top panels in Figures 2C to 2F show four representative spectra, expanded from the spectrum shown in Figure 2A, that led to the identification of the SERK1-interacting partner, 14-3-3ν. The peaks with *m/z* 1492.7 (Figure 2C) and 1611.8 (Figure 2E) are predicted with one phosphorylated residue present. The peak with *m/z* 1531.8 (Figure 2D) has the same predicted peptide sequence as that predicted for *m/z* 1611.8 (Figure 2E) but without phosphorylation of the Ser residue. The same peptide sequence, but now extended by two missed tryptic cleavage sites, is predicted for the peak with *m/z* 1716.8 (Figure 2F). The bottom panels in Figures 2C to 2F show the corresponding expanded spectra recorded for the negative control sample shown in Figure 2B.

The combined results of comparable analyses performed for the list of remaining *m/z* values (see supplemental material online) were used to compile the list of identified proteins; these are presented in Table 1. As expected, SERK1 was identified as part of the complex. This identification was based on 13 tryptic peptide matches and a Mascot score of 84. All of the peptides found covered the kinase domain of SERK1 and are located on the exterior of the protein, including the phosphorylated peptides, based on the structural model for SERK1 (Shah et al., 2001b). None of the peptides matched the sequence of the extracellular domain, which may be attributable to posttranslational modification by glycosylation (Shah et al., 2001a) or to the presence of two disulfide bounds between the four Cys residues present, making trypsin digestion more difficult. One peptide could be identified in which the oxidation of Met had occurred, whereas three other peptides were identified that were modified by phosphorylation. The second receptor in the SERK1 complex was identified as the SERK3 or BAK1 protein. LC/MALDI-TOF/MS fingerprint analysis revealed tryptic peptide *m/z* values from both SERK1 and SERK3, but because of the high homology in their protein sequences (78%), 8 of 13 of the predicted *m/z* values match with the sequences of both proteins. Five peptides unique for SERK3 were identified, three without and two with modification by phosphorylation. Based on inspection of the model of SERK1 structure, four of the five SERK3-specific peptides identified are from a region also yielding peptides used for the identification of SERK1. This finding corroborates the identification of SERK1 and SERK3.

For SERK2, which is 90% homologous with SERK1 at the protein level, five *m/z* values are identical for both proteins. No *m/z* values unique for SERK2 were found. The third receptor found in the SERK1 complex was the BRI1 receptor (Li and Chory, 1997) identified on the basis of 17 peptides, most of them covering the kinase domain. Most of the peptides identified with phosphorylations were also found as nonphosphorylated or as oxidized peptides, which provides additional evidence for identification as the BRI1 protein (see Supplemental Table 1 online). Because SERK3 (BAK1) is reported to be the coreceptor of BRI1 (Li et al., 2002; Nam and Li, 2002), the presence of both of these receptors suggests that there is a direct link between SERK1 activity and brassinolide signaling. In addition to SERK1, SERK3, and BRI1, several other proteins were found that were previously reported to interact with SERK1 and therefore were expected to be present in the SERK1 immunoprecipitated complex. One of them is *Arabidopsis* KAPP, which was shown to interact only with a catalytically active kinase domain of SERK1, involving Thr-468 (Shah et al., 2001b).

In a yeast two-hybrid screen, two other proteins were found to interact with the kinase domain of SERK1, CDC48A and 14-3-3λ (Rienties et al., 2005). MALDI-TOF/MS fingerprint analysis indeed revealed tryptic peptides derived from CDC48A (Table 1). In our search, 14-3-3ν, rather then 14-3-3λ, was identified with a high score after searching even with the complete *m/z* list. Apparently, only these two members of the large *Arabidopsis* family of 14-3-3 proteins can interact with the SERK1 receptor. Finally, two unexpected proteins were found. The first is the MADS box transcription factor AGL15 (Heck et al., 1995), and the second is a putative CONSTANS (CO)-like B-box zinc finger protein (At2g33500). The zinc finger protein is annotated as one large 401–amino acid protein and also as a shorter protein of 186 amino acids. We only found peptides covering the shorter protein. To validate that the proteins described above indeed interacted with SERK1, we treated control samples with SDS or with 0.5 M NaCl before coimmunoprecipitation to destroy protein–protein interactions. The resulting list of *m/z* values revealed only the presence of the SERK1 protein (data not shown). Finally, we used our coimmunoprecipitation procedure with the GFP-tagged BRI1 receptor and the GFP-tagged integral membrane protein PIN1. For BRI1, the resulting *m/z* lists did not reveal the presence of any of the SERK1-interacting proteins listed in Table 1 (data not shown). Therefore, we conclude that the coimmunoprecipitation/LC/MALDI-TOF/MS procedure for identifying protein complexes in *Arabidopsis* presented here is reliable and identifies specific interacting partners.

BRI1, SERK3, CDC48A, and 14-3-3ν Interact in Vivo with SERK1

To confirm our results obtained by LC/MALDI-TOF/MS, we used coimmunoprecipitation and FLIM-based analysis to detect the interaction between SERK1 and its interacting partners in vivo. CFP-tagged SERK1 was immunoprecipitated with anti-GFP antibodies, and the precipitated proteins were detected using anti-BRI1 antibodies. A band with the expected mobility of BRI1 was visualized (Figure 3A, lane 1) that was absent in an immunoprecipitation of wild-type plants with the GFP antibody (Figure 3A, lane 2). BRI1 antibodies recognize endogenous BRI1 as well as BRI1-GFP fusion proteins and can precipitate BRI1 from a total plant protein extract (Figure 3B, lanes 1 to 3). The BRI1 antibodies are specific for BRI1 because they do not detect a band of the expected mobility for BRI1 in a protein extract from seedlings of the strong *bri1-4* allele (data not shown). Reciprocal coimmunoprecipitation with anti-BRI1 antibodies revealed the presence of SERK1-CFP in the coimmunoprecipitated proteins (Figure 3C, lane 1).

Previously, we showed that FRET can be detected between CFP and YFP of SERK3 and BRI1 when transiently expressed in cowpea (*Vigna unguiculata*) protoplasts. Coexpression of BRI1 and SERK3 results in a change of the steady state distribution of both receptors as a result of accelerated endocytosis (Russinova

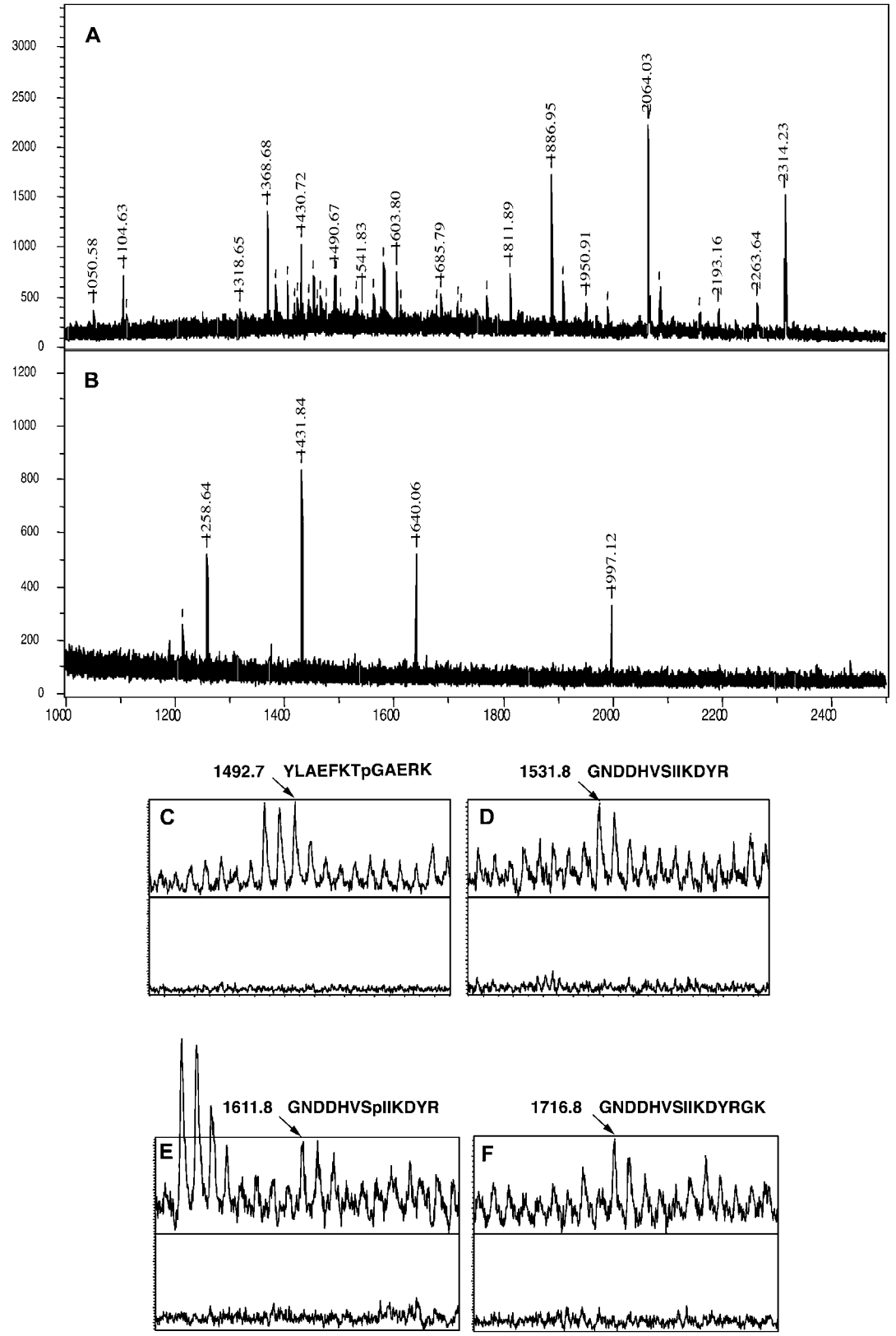

Figure 2. LC/MALDI-TOF/MS Spectra Obtained after Trypsin Digestion of SERK1-GFP Immunoprecipitated Complex.

Table 1. SERK1-Interacting Proteins Identified by MALDI-TOF/MS

Protein Name	At Number	Number of Peptides Identified	Sequence Coverage (%)	Mascot Score Obtained	Protein Size (kD)	Conformation from Additional Experiments
SERK1	At1g71830	13	15	84	69	IP
SERK3	At4g33430	13	17	96	68	FRET
BRI1	At4g39400	17	9	76	130	CoIP, FRET
KAPP	At5g19280	18	25	102	65	FRET, Y2H
CDC48A	At3g09840	14	19	80	89	CoIP, Y2H, FRET*
14-3-3ν	At3g02520	12	23	110	30	CoIP
AGL15	At5g13790	7	37	62	30	ND
Zinc finger protein	At2g33500	11	45	195	21	ND

The proteins identified in the SERK1 complex all have MASCOT scores of >60 and were grouped according to postulated function. Interactions were confirmed using coimmunoprecipitation (CoIP), or in the case of SERK1 alone by immunoprecipitation (IP), yeast two-hybrid interaction (Y2H) (Rienties et al., 2005), and detection of FRET, which is indicative of protein proximity in transient protoplast transfection assays (Shah et al., 2002; Rienties et al., 2005; this study). ND, not determined. The asterisk indicates unpublished data (J. Aker, E. Russinova, and S. de Vries).

et al., 2004). To determine whether SERK1 can form heterodimers with either BRI1 or SERK3 in the plasma membrane, we used a similar transient assay in protoplasts to detect FRET by FLIM. In Figure 3D, we show the fluorescence intensity images of protoplasts transfected with SERK1-CFP alone (Figure 3D, I), SERK1-CFP together with BRI1-YFP (Figure 3D, II), and SERK1-YFP together with SERK3-CFP (Figure 3D, III). The corresponding fluorescence lifetime images are compared in panels IV to VI in Figure 3D. The results presented in Figure 3D (panel V) show that SERK1 and BRI1 heterodimerize in small patches in the plasma membrane, as indicated by the significant reduction in the average lifetime (τ) from 2.5 to 2.1 ns of the donor (SERK1-CFP) molecules in those areas indicated by the arrowhead. A similar phenomenon was described for the SERK3/BRI1 heterodimers (Russinova et al., 2004). SERK1-YFP also formed heterodimers with SERK3-CFP in the plasma membrane, as shown by the green plasma membrane in Figure 3D (panel VI) that corresponds to an average lifetime of 1.9 ns for the donor (SERK3-CFP) molecules. Thus, colocalization in the plasma membrane and the ability to form heterodimers in plant protoplasts strongly suggest that SERK1, SERK3, and BRI1 can be part of the same complex in intact plant membranes.

To confirm the in vivo interaction of CDC48A with SERK1, we coimmunoprecipitated SERK1 from *Arabidopsis* tissue-cultured cells with anti-GST-SERK1 kinase antibodies (Rienties et al., 2005). The precipitated proteins were analyzed by immunoblotting using anti-CDC48 antibodies (Rancour et al., 2002). A band with the expected mobility for monomeric CDC48A was detected in the total protein extract (Figure 4A, lane 1) and in the immunoprecipitated sample (Figure 4A, lane 3), showing that *Arabidopsis* CDC48A indeed coimmunoprecipitates with SERK1. No CDC48A band was detected in the negative control using rabbit preimmune serum for immunoprecipitation (Figure 4A, lane 2). Similarly, the presence of a 14-3-3 protein in the complex with SERK1 in vivo was verified by coimmunoprecipitation with GFP antibodies of CFP-tagged SERK1 followed by immunodetection with anti–14-3-3 antibodies (Figure 4B, lane 1). No 14-3-3 band was detected in the negative control using wild-type seedlings for immunoprecipitation (Figure 4B, lane 2). The 14-3-3 antiserum can recognize in vitro–produced 14-3-3ν (data not shown) as well as 14-3-3λ, confirming that SERK1 can interact with both 14-3-3λ (Rienties et al., 2005) and 14-3-3ν isoforms. A summary of the experiments providing additional evidence for the presence of proteins in the SERK1 complex is shown in Table 1.

SERK1 Interacts Genetically with BRI1

Analysis of the single T-DNA insertion mutant *serk1-1*, an allele that produces a kinase-dead receptor protein, did not reveal a morphological plant phenotype (Albrecht et al., 2005). Therefore, we crossed the *serk1-1* allele into the weak BRI1 mutant allele *bri1-119*. This allele contains the G644D missense mutation in the island domain of BRI1 (Friedrichsen et al., 2000). At the seedling level, 7-d-old *bri1-119* mutants exhibit mild morphological characteristics of the phenotype conferred by *bri1*, such as small seedlings, short petioles, and round, dark green, inwardly curved true leaves (Figure 5A). *bri1-119* plants developed smaller, compact rosettes (Figure 5D) compared with wild-type plants. The weak *bri1-119* allele is a semifertile dwarf that has less reduced stature (Figure 5D) compared with severe *bri1*

Figure 2. (continued).

(A) and **(B)** MALDI-TOF/MS spectra from SERK1-CFP immunoprecipitated complex **(A)** (fraction 9 of 24) compared with the corresponding spectra (fraction 9) from the control immunoprecipitation performed with wild-type plants **(B)**. The spectra were obtained after LC separation from the trypsin-digested proteins after immunoprecipitation. The *x* axis represents *m/z* values. The *y* axis represents the intensity of the peaks in arbitrary units.
(C) to **(F)** Four representative spectra expanded from **(A)** (top panels) and **(B)** (bottom panels), which led to the identification of one of the SERK1-interacting partners, 14-3-3ν. The corresponding predicted peptides are also shown. The peaks are present only in the spectra from SERK1-CFP immunoprecipitation (top panels) and not in the controls (bottom panels).

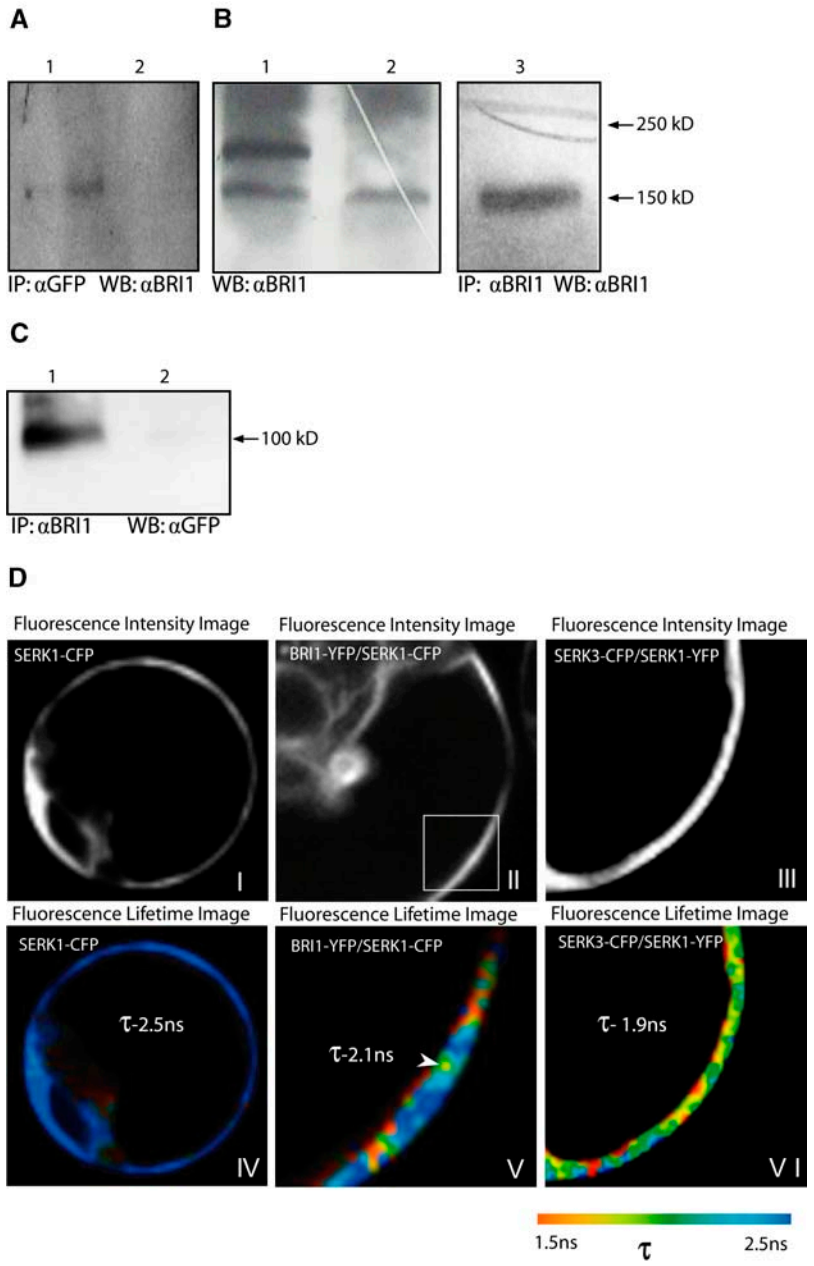

Figure 3. Direct Interaction of SERK1 with BRI1 and SERK3.

(A) Total protein extract from SERK1-CFP transgenic seedlings was immunoprecipitated using anti-GFP antibodies (lane 1). As a negative control, proteins extracted from wild-type plants were precipitated using anti-GFP antibodies (lane 2). WB, protein gel blot.

(B) Total protein extracts from BRI1-GFP transgenic seedlings (lane 1) and wild-type (lane 2) and immunoprecipitated (lane 3) products from wild-type seedlings were separated on an 8% SDS-PAGE gel and detected using anti-BRI1 antibodies.

(C) A protein extract from SERK1-CFP transgenic plants was precipitated using anti-BRI1 antibodies (lane 1). As a negative control, a protein extract from wild-type plants was precipitated with the same antibodies (lane 2).

The resulting immunoprecipitates were separated by 8% SDS-PAGE, transferred to a membrane, and probed with anti-GFP antibodies for detection of SERK1-CFP fusion proteins **(C)** or with anti-BRI1 antibodies for detection of BRI1 protein (**[A]** and **[B]**). Arrows indicate the sizes of the marker proteins. IP, immunoprecipitate.

(D) FRET between SERK1, SERK3, and BRI1 imaged by FLIM on cowpea protoplasts transiently expressing SERK1-CFP (I and IV), BRI1-YFP/SERK1-CFP (II and V), and SERK3-CFP/SERK1-YFP (III and VI) for 16 h. Fluorescence intensity images representing steady states of the donor SERK1-CFP or SERK3-CFP fluorescence are presented in I to III. Mean fluorescence lifetime values (τ) and lifetime distribution for the images in I to III are presented as pseudocolor images in IV to VI, respectively. The arrowhead points to an area with a short lifetime, indicative of FRET. Note the color bar, where dark blue is used to show a τ of 2.5 ns (no interaction) and light green is used to show a τ of 1.9 ns (interaction). The red to dark orange areas corresponding to a τ of 1.5 ns are attributable to autofluorescence effects.

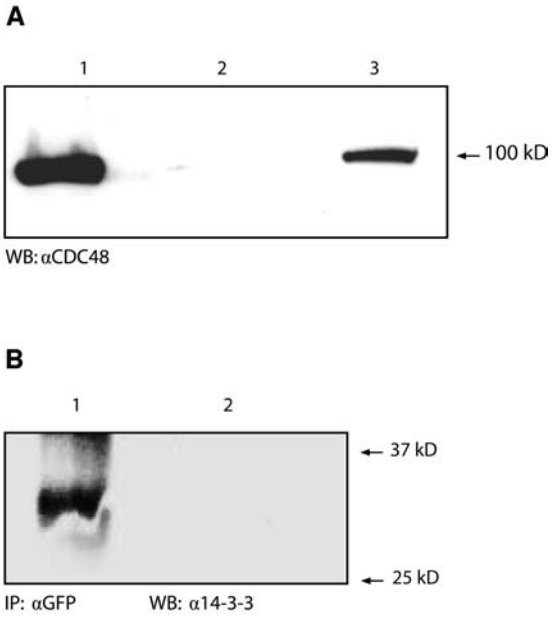

Figure 4. SERK1 Interacts in Vivo with *Arabidopsis* CDC48A and 14-3-3.

(A) Coimmunoprecipitation of SERK1 and CDC48A. Total protein extract was isolated from *Arabidopsis* tissue cell culture, analyzed directly by SDS-PAGE, and immunodetected with anti-CDC48 antibody (lane 1), or immunoprecipitated with anti-SERK1 kinase antibody (lane 3) or preimmune serum (lane 2) and detected with anti-CDC48 antibody.
(B) Coimmunoprecipitation of SERK1 and 14-3-3. Total protein extract was isolated from SERK1-CFP transgenic plants (lane 1) or wild-type plants (lane 2) and precipitated with anti-GFP antibody. Precipitated proteins were immunodetected with anti–14-3-3 antibodies.
The sizes of the marker proteins are indicated by arrows. IP, immunoprecipitate.

alleles (Noguchi et al., 1999). The *serk1-1* mutation clearly enhanced all BRI1-associated phenotypes, especially the length of the petioles and excessive inward curling, now seen in 7-d-old seedlings of the double mutant *bri1-119 serk1-1* (Figure 5B), as well as a reduction in the size of the rosette (Figure 5E; see Supplemental Table 2 online). The inflorescence length of the double *bri1-119 serk1-1* mutant was also reduced (Figure 5H; see Supplemental Table 2 online). For comparison, we also introduced the *serk3* mutation (Russinova et al., 2004), an allele of the BAK1 coreceptor, into *bri1-119*. The resulting *bri1-119 serk3* double mutant had even smaller rosettes (Figure 5F) and grew with a severely reduced stature (Figure 5I; see Supplemental Table 2 online) resembling strong *bri1* alleles. This finding indicates that the *serk3* mutation had an even stronger effect on *bri1-119* than did *serk1-1*. To rule out the possibility that the observed modification of the phenotype conferred by *bri1-119* by the *serk1-1* allele is attributable to the introduction of the Columbia ecotype into the Enkheim-2 background, we also combined the *serk2-2* mutant allele, which shows no morphological alterations from the wild type (Albrecht et al., 2005), with *bri1-119* (see Supplemental Table 2 online). The resulting *bri1-119 serk2-2* double mutants were indistinguishable from *bri1-119* in terms of inflorescence length and rosette width, demonstrating that there is no effect of the Columbia ecotype. These results provide genetic evidence that SERK1 is involved in BRI1 signaling and confirm the role of the *SERK3* (*BAK1*) gene as a BRI1 coreceptor.

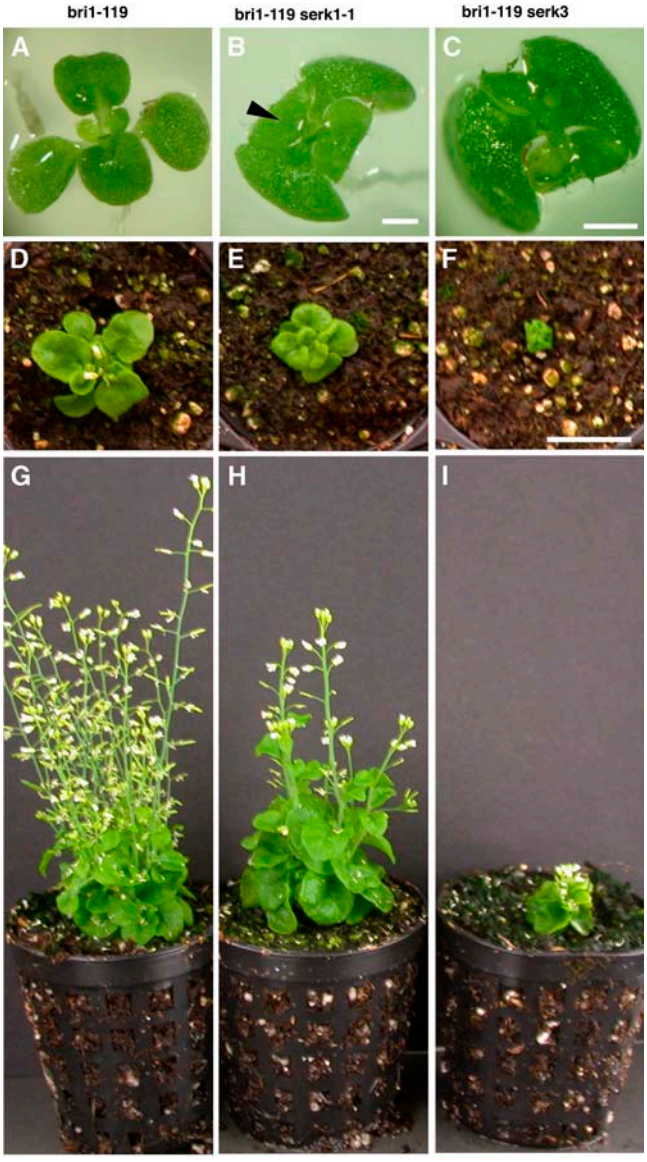

Figure 5. SERK1, SERK3, and BRI1 Function Together.

serk1-1 and *serk3* mutations enhance the weak *bri1-119* mutation. Seven-day-old seedlings are shown in **(A)** to **(C)**, 3-week-old plants are shown in **(D)** to **(F)**, and 6-week-old plants are shown in **(G)** to **(I)**. **(A)**, **(D)**, and **(G)** show *bri1-119*, **(B)**, **(E)**, and **(H)** show *bri1-119 serk1-1*, and **(C)**, **(F)**, and **(I)** show *bri1-119 serk3* mutations. Note the increase in the curliness of the first true leaves and the reduction in the petiole length in the double mutant seedlings as well as the reduced rosette width of the double mutant plants. Bars = 1 mm in **(B)** and **(C)** and 2 cm in **(F)**.

Identification of a Membrane-Associated SERK1-Containing Complex Using Blue Native PAGE

In previous studies, we showed that SERK1 is located at the membrane in protoplasts and in plants (Russinova et al., 2004; Kwaaitaal et al., 2005) and can directly interact in vitro and in vivo with KAPP and 14-3-3λ and in vitro with CDC48A (Shah et al., 2002; Rienties et al., 2005). The results presented here confirm the previously observed interactions and show that SERK1 can be present in a complex with several other proteins. It is not clear whether the SERK1 complex harbors all of the proteins listed in Table 1 at the same time or that we immunoprecipitated multiple forms of the SERK1 complex. Different forms could exist in different cell types or in different subcellular locations, such as plasma membrane or after internalization (Russinova et al., 2004). To determine the size of the SERK1 complex in planta, microsomal preparations from SERK1-CFP– and BAK1-GFP–expressing seedlings and wild-type seedlings were solubilized with Triton X-100 and subjected to blue native (BN) PAGE. In this technique, Coomassie dyes and aminocaproic acid are used to induce a charge shift and improve the solubilization of membrane-associated proteins (Rivas et al., 2002). To detect SERK1 within the potential protein complex, single lanes of the BN-PAGE gel were cut and mounted on a denaturing SDS gel. After electrophoresis, the gel was subjected to immunoblot analysis using anti-GFP antibody or anti-GST-SERK1 kinase antibody. Using mass standards, ~85% of the protein complex containing SERK1 was determined to have a mean relative mass of 350 kD. The remaining 15% appears to exist as a complex with a mean mass of 450 kD. The maximum size is ~500 kD (Figure 6A). This variability in protein complex size is also seen when the tagged SERK1-CFP complex is detected by anti-GFP antibodies (Figure 6B). Approximately 90% of the CFP-tagged complex has a mean mass of 400 kD and 10% has a mass of ~500 kD. Although there is a clear difference in the mean size of the complex with and without the CFP tag, we cannot precisely estimate whether this difference is 25 kD (one molecule of CFP protein) or 50 kD (two molecules of CFP protein).

The results show that there is one abundant core complex for SERK1 of ~350 kD. We first examined whether BRI1 was part of the core SERK1 complex. Therefore, a microsomal fraction prepared from SERK1-CFP transgenic plants was examined for the presence of BRI1 proteins. BRI1 was found in complex with the same size range of 400 to 500 kD (Figure 6C, panel 1) as the SERK1-CFP proteins. In contrast with SERK1, most of the BRI1 protein was found as probably a homodimeric form of ~250 kD (Figure 6C, panel 2). The occurrence of potential BRI1 homodimers is consistent with our observation of BRI1 homodimerization in protoplast (Russinova et al., 2004) and was recently shown in plants (Wang et al., 2005b). The observed smaller and higher forms of BRI1 are probably attributable to the recognition of differentially processed forms (Figure 6C). The distribution of BAK1 in the microsomes prepared from BAK1-GFP transgenic plants was then studied by BN-PAGE. BAK1-GFP was found in complex(es) with the same size range as SERK1-CFP (Figure 6D). These data suggest that BRI1, SERK1, and SERK3 are indeed present in the main 350-kD core complex and are also present in complexes of higher molecular mass. No signal was detected when solubilized microsomes from wild-type seedlings were analyzed for the presence of GFP, confirming that the signals observed in Figures 6B and 6D are indeed derived from microsomal SERK1-CFP or BAK1-GFP (Figure 6E). Collectively, the results obtained from BN-PAGE suggest that the core SERK1

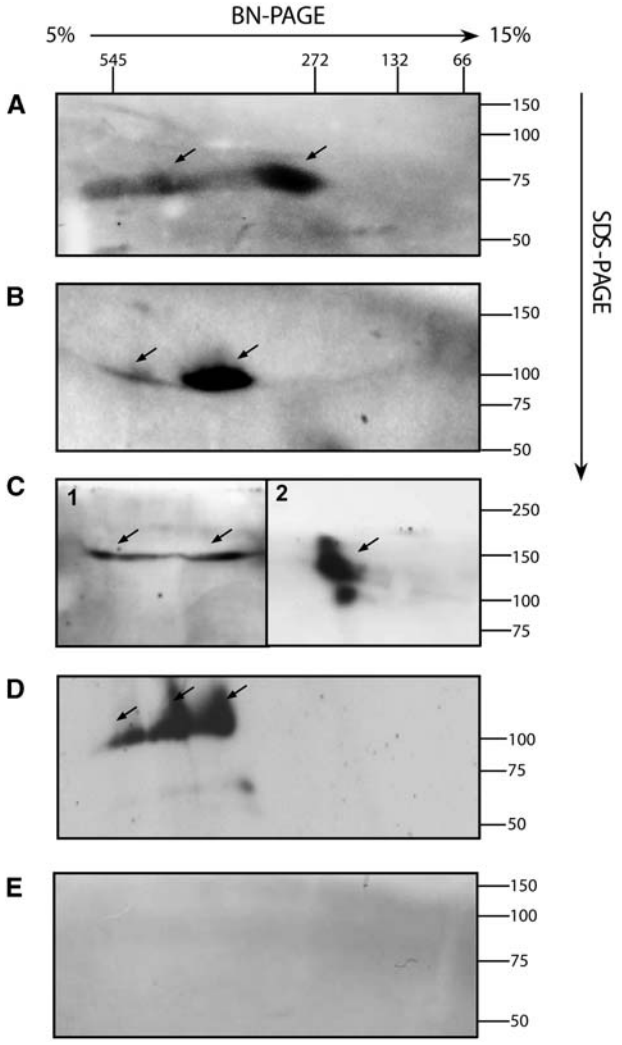

Figure 6. BN-PAGE of Solubilized Wild-Type and SERK1-CFP Microsomes.

Microsomes were isolated from wild-type plants (**[A]** and **[E]**) and SERK1-CFP–expressing (**[B]** and **[C]**) or BAK1-GFP–expressing **(D)** transgenic plants and subjected to BN-PAGE in the first dimension and SDS-PAGE in the second dimension. Proteins were immunodetected using anti-SERK1 kinase antibodies **(A)**, anti-GFP antibodies (**[B]**, **[D]**, and **[E]**), or anti-BRI1 antibodies **(C)**. In **(C)**, panel 1 shows part of the membrane exposed for 3 h, and 2 shows part of the same membrane exposed for 3 min. The molecular masses of standard proteins used are indicated at top (BN-PAGE) and at right (SDS-PAGE). Arrows in **(A)** indicate the positions of the main SERK1 complex sizes of 350 and 450 kD, and arrows in **(B)** indicate the positions of the main SERK1-CFP complexes of 400 and 500 kD. Arrows in **(C)** indicate the positions of the main BRI1 complexes of 250, 350, and 450 kD, and arrows in **(D)** indicate the main BAK1-GFP complexes ranging from 350 to 450 kD.

complex of ~350 kD as well as the larger complexes consist of the membrane receptors SERK1, SERK3, and BRI1. Assuming that all proteins listed in Table 1 are present as monomers, a predicted size of ~500 kD is obtained. Although this is about the maximum size of the SERK1 complex as estimated by BN-PAGE, it exceeds the size of the predominant complex of 350 kD.

In summary, we propose that in *Arabidopsis* seedlings, a core SERK1 membrane complex consists of SERK1, BRI1, and SERK3. Collectively, this would amount to ~270 kD when all proteins are present as monomers, or between 350 and 400 kD in a more conventional tetrameric arrangement. This is clearly in the range of the observed sizes on BN-PAGE gels. KAPP interacts only with the active SERK1 receptor (Shah et al., 2002) and could represent one of the less abundant higher molecular mass forms.

DISCUSSION

In this work, we used a combination of coimmunoprecipitation based on the GFP variant CFP as a protein tag and LC/MALDI-TOF/MS to identify proteins associated with the membrane receptor SERK1. Based on our data with other membrane proteins from *Arabidopsis*, this technique appears to be of general use. Compared with other techniques to identify interacting proteins, such as in vitro pulldown assays and yeast two-hybrid screens, the main advantage is that the immunoprecipitation combined with LC/MALDI-TOF/MS allows protein complex isolation under native conditions, therefore allowing functional studies in which the activity or posttranslational modification of one or several proteins in the complex can be examined (Drewes and Bouwmeester, 2003). Another advantage is that the CFP tag allows one to directly follow all subcellular localizations of the fusion proteins. This allows predictions concerning the nature of the proteins recovered, especially in the case of membrane receptors undergoing recycling (Russinova et al., 2004). Other tags have been used, such as tandem affinity purification tags for plant protein complex isolation in a transient expression system or in stably transformed transgenic lines, using the cauliflower mosaic virus 35S promoter (Rohila et al., 2004; Rubio et al., 2005). Our procedure differs in several respects: we used an endogenous promoter-based construct and only used CFP as a protein tag, thereby minimizing potential biological problems arising from the use of strong constitutive promoters. Also, we used integral membrane protein as a bait, rather than the soluble proteins used previously.

SERK1 and BR Signaling

A highly interesting finding was the identification of two members of the BR signaling pathway, the main BR receptor BRI1 (Li and Chory, 1997) and its coreceptor BAK1 (SERK3) (Li et al., 2002; Nam and Li, 2002), as components of the SERK1 complex. This finding implies that SERK1 is a previously unrecognized element of BR signaling. Recently, we showed that the SERK3 receptor may have a role in the internalization of BRI1 after heterodimerization and that BRI1 can also form homodimers in the plasma membrane (Russinova et al., 2004). Further biochemical evidence comes from the finding here that BRI1 and SERK1 as well as SERK1 and SERK3 can interact in the plasma membrane of protoplasts. FRET studies between SERK1-CFP and SERK1-YFP have shown that only 15% of SERK1 exists as homodimers on the plasma membrane of protoplast cells (Shah et al., 2001a). Our results showed that both SERK1 and SERK3 heterodimerize with the BRI1 receptor, suggesting that both coreceptors can have comparable activity in terms of BRI1 signaling and/or internalization. Another piece of evidence is that a *bak1* null allele shows less severe phenotypes than *bri1* loss-of-function alleles, indicating that partially redundant activity could be attributed to different SERK family members (Li et al., 2002; Nam and Li, 2002). Genetic analysis of the *serk1-1 bri1-119* double mutant suggests that SERK1–BRI1 interactions indeed affect BRI1-mediated signaling in planta, but to a lesser extent than SERK3–BRI1 interactions. Notably, none of the proposed downstream components of BRI1, such as BES1, BZR1, or BIN2 (Li and Nam, 2002; Wang et al., 2002b; Yin et al., 2002), was detected in the SERK1 complex.

It is unlikely that all proteins (as identified by MALDI-TOF/MS) listed in Table 1 are present in a complex together with SERK1 at the same time. Especially because proteins such as receptors and CDC48A (Rancour et al., 2002, 2004) are known to shuttle between monomeric and multimeric forms and can change their interaction properties upon activation and relocalization, multiple forms of the same complex are to be expected. An indication of the presence of different complexes is the localization of SERK1 in the plasma membrane as well as in internalized membrane compartments (Russinova et al., 2004; Kwaaitaal et al., 2005).

It was proposed that BRI1 forms heterodimers with SERK3 to initiate BR signaling upon BR binding (Li et al., 2002; Nam and Li, 2002). This was recently confirmed in an elegant demonstration of the in vivo phosphorylation properties of the BRI1 receptor (Wang et al., 2005a). In that work, it was clearly shown that the interaction between the BAK1 (SERK3) proteins and BRI1 is brassinolide-dependent. Because we did not apply exogenous ligands before isolation of the SERK1 complex, it is likely that only a small fraction of the complexes we isolated are actively signaling via the SERK1 protein. This notion seems to be supported by the fact that most of the BRI1 receptors were unassociated with SERK1 in seedlings. Although our results do not allow us to precisely predict the composition, it is likely that SERK1, SERK3, and BRI1 receptors can form tetrameric complexes analogous to the functional complex of transforming growth factor-β (TGF-β) receptors. Each type of TGF-β receptor is also present as a ligand-independent dimer on the cell surface. TGF-β binding to the TβRII homodimers promotes the formation of $(T\beta RI)_2/(T\beta RII)_2$ heterodimers, in which TβRI is phosphorylated by the constitutively active TβRII and becomes activated to propagate the TGF-β signal. Combinatorial interactions in the tetrameric receptor complex allow differential ligand binding or differential signaling in response to the same ligand. One receptor combination often binds different ligands, and patterns of ligand and receptor expression dictate which receptor–ligand combination is activated (Feng and Derynck, 1997). This so-called tetrameric model was also recently proposed for BRI1 and BAK1 (SERK3) (Wang et al., 2005b).

Other SERK1 Complex Components

The presence of the PP2C phosphatase KAPP, 14-3-3ν, and CDC48A in the SERK1 complex confirms previously obtained results using yeast two-hybrid screening and in vitro interaction studies (Rienties et al., 2005). Collectively, these proteins appear to be involved in dephosphorylation, protein interaction and membrane interaction, and protein degradation, respectively. It is likely that they represent receptor maintenance or trafficking functions. Previously, it was shown that SERK1 could interact with 14-3-3λ (Rienties et al., 2005). The results presented here suggest that the receptor preferentially interacts with 14-3-3ν in seedlings and perhaps with 14-3-3λ in siliques, given the origin of the *Arabidopsis* cDNA library from young silique tissue that was used for yeast two-hybrid screening. The kinase domain of SERK1 is able to transphosphorylate and bind in vitro to CDC48A, 14-3-3λ, and KAPP (Rienties et al., 2005). In vitro, the interactions are all phosphorylation-dependent. In vivo, it was shown that SERK1 interacts with KAPP only in intracellular vesicles, and it was proposed to play a role in receptor internalization as well as in dephosphorylation (Shah et al., 2002). For two other LRR-RLKs, CLV1 (Williams et al., 1997) and FLS2 (Gomez-Gomez et al., 2001), it has been shown that KAPP functions as a negative regulator, and it may have the same role in controlling signaling through the SERK1 receptor.

CDC48 protein assembles mainly in hexameric forms (Rancour et al., 2002). In *Arabidopsis* suspension-cultured cells, soluble (cytosolic) CDC48A was found in a high molecular mass protein of 640 kD. Recently, it was proposed that CDC48A interacts with PUX1 as a monomer and may function in regulating plant growth (Rancour et al., 2004) and also in the plant endoplasmic reticulum–associated protein degradation system (Muller et al., 2005).

Plant 14-3-3 proteins have also been found associated with G-box transcription factors (Lu et al., 1992). Five *Arabidopsis* 14-3-3s, including 14-3-3λ, have been shown to interact with other transcription factors (Pan et al., 1999), and current models propose that the interaction with members of the 14-3-3 family is client-driven (Paul et al., 2005).

Two transcription factors were found to be associated with the SERK1 complex: AGL15 and a putative CO-like B-box zinc finger protein. Most likely, these two proteins do not interact directly with the receptor but require 14-3-3 proteins as adaptor proteins. It has been shown that 14-3-3 proteins can also promote the cytoplasmic localization or, conversely, the nuclear localization, of transcription factors (reviewed in Muslin and Xing, 2000). One of the other MADS box transcription factors, AGL24, was shown to interact directly with the kinase domain of the *Arabidopsis* meristematic receptor-like kinase and to be phosphorylated by the kinase domain of the receptor in vitro (Fujita et al., 2003). AGL15 was shown to accumulate in nuclei but also to be present in the cytoplasm (Perry et al., 1996). SERK1 and AGL15 are highly expressed during embryogenic cell formation in culture and during early embryogenesis. As found for SERK1 (Hecht et al., 2001), AGL15 promotes somatic embryo production from the shoot apical meristem in liquid culture when ectopically overexpressed (Perry et al., 1996; Harding et al., 2003). Interestingly, AGL15-overexpressing tissues also had increased expression of SERK1 (Harding et al., 2003). It was shown that AGL15 could bind directly to the promoter regions of different targets (Wang et al., 2002a). Those authors described how after chromatin immunoprecipitation, they obtained DNA fragments containing *cis*-regulatory elements targeted by AGL15, which may contribute to the regulation of the *SERK* gene by directly binding to its promoter. These data and our findings suggest that SERK1 and AGL15 can be involved in the same signaling pathway.

The other putative transcription factor found in the SERK1 complex belongs to a large family of CO-like zinc finger transcription factors, in which the zinc finger region regulates protein–protein interactions, as found for several animal transcription factors (reviewed in Griffiths et al., 2003). Recently, it was shown that CO accumulation is regulated by photoreceptors in photoperiodic flowering (Valverde et al., 2004).

In conclusion, we propose that in *Arabidopsis* seedlings, signaling mediated by the SERK1 receptor combines elements of the BR pathway with a short signal transduction chain, in which the plasma membrane receptor is in a complex with its cognate transcriptional regulators, such as AGL15. Further studies are needed to evaluate this model and to map the phosphorylation sites that are responsible for the activation of receptor kinases and the recruitment of downstream signaling components.

METHODS

Plant Materials and Growth Conditions

Arabidopsis thaliana ecotype Columbia was used as the wild type. Seeds were surface-sterilized and sown on germination medium (half-strength Murashige and Skoog salt and vitamins medium [Duchefa] supplemented with 0.8% [w/v] agar [Daishin] and 2% [w/v] sucrose). Seeds were kept for 2 d at 4°C and then transferred to a growth chamber. Seedlings were grown at 22°C under 16-h light/8-h dark periods for 7 d. *Arabidopsis* plants expressing the SERK1 receptor fused to CFP under the control of its native promoter were similar to the SERK1-YFP–expressing plants described previously by Kwaaitaal et al. (2005). BRI1-GFP transgenic plants used for immunoprecipitation and BAK1-GFP plants used for BN-PAGE were described previously (Nam and Li., 2002; Russinova et al., 2004). The *bri1-4* strong allele (No. 3953; obtained from Frans Tax via the Arabidopsis Stock Center) was described previously by Noguchi et al. (1999).

Generation of *bri1-119 serk1-1*, *bri1-119 serk3*, and *bri1-119 serk2-2* Double Mutants

The *bri1-119* mutant was obtained from the ABRC (Ohio State University; stock No. CS399, ecotype Enkheim-2) and was described previously by Noguchi et al. (1999) and Friedrichsen et al. (2000). The SERK1 and SERK3 knockout lines, *serk1-1* and *serk3*, were obtained from the SIGnAL TDNA-Express collection (Alonso et al., 2003) as insertion lines SALK_544330 and SALK_034523.56.00, respectively, and the *serk2-2* insertion line (No. 119-G03) was from the Syngenta *Arabidopsis* insertion lines, described previously by Albrecht et al. (2005), in the Columbia background. *bri1-119 serk1-1* and *bri1-119 serk2-2* were generated by crossing *bri1-119* with *serk1-1* or *serk2-2*, respectively; *bri1-119 serk3* was generated by crossing *bri1-119* with *serk3*. In each case, F1 plants were allowed to self-fertilize, and candidate double F2 plants were genotyped phenotypically and by PCR.

Transient Expression in Protoplasts and FLIM

The full-length SERK1, SERK3, and BRI1 CFP and YFP fusion constructs were described previously (Shah et al., 2001a; Russinova et al., 2004). FLIM was performed using a Bio-Rad Radiance 2100 MP system in combination with a Nikon TE 300 inverted microscope as described (Russinova et al., 2004). From the intensity images obtained, complete fluorescence lifetime decays were calculated per pixel and fitted using a double exponential decay model. The fluorescence lifetime of one component was fixed to the value found for SERK1-CFP (2.5 ns).

Protein Extraction, SDS-PAGE, and Protein Gel Blot Analysis

To prepare total protein extracts, plant material was ground in liquid nitrogen and thawed in extraction buffer containing 50 mM Tris, pH 7.5, 150 mM NaCl, 0.5% Triton X-100, and a protease inhibitor cocktail according to the manufacturer's instructions (Roche). Samples were incubated on ice for 30 min. The suspension was centrifuged at 200*g* (Beckman Microfuge 18 centrifuge) at 4°C for 3 min. The concentration of extracted proteins was determined with the Bio-Rad protein assay. After boiling 30 μg of total protein for 5 min in sample buffer containing 100 mM Tris-HCl, pH 6.8, 4% SDS, 0.2% bromphenol blue, 20% glycerol, and 100 mM DTT, the proteins were separated on 8 or 12% SDS-polyacrylamide gels (Laemmli, 1970) and transferred onto nitrocellulose (Schleicher & Schuell) by wet electroblotting (Mini-Protean II system; Bio-Rad). Proteins were analyzed by immunoblotting with anti-GFP (IgG fraction, 1500× dilution; Molecular Probes), and a polyclonal antibody was generated against the GST-SERK1 kinase domain fusion protein (3000× dilution) (Rienties et al., 2005). Anti-BRI1 specific antibodies were kindly provided by Joanne Chory (Salk Institute for Biological Studies; used at 1000× dilution), anti-CDC48A antibodies (Rancour et al., 2002) were kindly provided by Sebastian Bednarek (Department of Biochemistry, University of Wisconsin; used at 1000× dilution), and-14-3-3 antibodies have been described previously (Rienties et al., 2005). Bound primary antibodies were detected with horseradish peroxidase–conjugated IgG purified donkey anti-rabbit secondary antibody at 10,000× dilution (Rockland Laboratories) or goat anti-chicken secondary antibody at 5000× dilution (Rockland Laboratories) and visualized using reagents for chemiluminescent detection (ECL Plus reagent; Amersham Biosciences).

BN-PAGE

Preparation of microsomes and BN-PAGE were performed as described (Rivas et al., 2002). Microsomes from 7-d-old seedlings from wild-type plants or transgenic plants expressing the SERK1 promoter-SERK1-CFP construct were solubilized in extraction buffer supplemented with 750 mM aminocaproic acid and incubated for 30 min on ice. Aliquots of supernatants were incubated with 0.5% Coomassie Brilliant Blue G 250 and 5% (v/v) glycerol and loaded on the gel. BN-PAGE was then performed according to Schagger and von Jagow (1991) on a 5 to 15% gradient polyacrylamide gel. Albumin bovine monomer (66 kD), albumin bovine dimer (132 kD), urease trimer (272 kD), and urease hexamer (545 kD) from Sigma-Aldrich were used as marker proteins.

Immunoprecipitations

Routinely, we used four plates (9 cm) with ~400 7-d-old seedlings (100 per plate) to prepare a protein extract suitable for immunoprecipitation. Ten milliliters of total plant protein extract (1 mg/mL) in extraction buffer (isolated as described above) was incubated for 1 h at 4°C with 100 μL of 50% (v/v) protein A–Sepharose CL-4B beads slurry (Amersham Biosciences) in 50 mM Tris and 150 mM NaCl, pH 7.5. After centrifugation at 200*g* (Beckman Microfuge 18 centrifuge) for 2 min at 4°C, the supernatant was incubated with 7 μL of anti-GFP, anti-BRI1, anti–14-3-3, anti-CDC48A, or rabbit preimmune serum. After incubation with gentle mixing for 1 h at 4°C, 200 μL of fresh 50% slurry of protein A beads was added, and incubation was continued for 4 h. Protein A beads were pelleted by centrifugation at 200*g* for 1 min, and the supernatant was removed. The beads were washed three times with 1 mL of wash buffer (50 mM Tris, pH 7.5, and 150 mM NaCl) and once with 10 mM NH_4HCO_3, pH 8. Before the last wash step, the beads together with the wash buffer were moved to a new tube. After centrifugation, the wash buffer was removed, and the beads were used in this form directly for digestion with trypsin and subsequent MALDI-TOF/MS analysis.

For immunodetection, the proteins were eluted from the beads by adding SDS sample buffer and boiling for 5 min at 95°C. In the case of coimmunoprecipitation of SERK1-CFP with rabbit anti-GFP antibodies and detection with rabbit anti–14-3-3 antibodies, no DTT was included in the SDS sample buffer. This prevents separation of the heavy and light chains of the antibodies and improves the resolution of the blots, because the detection system also recognized IgGs whose light chains overlap with the 14-3-3 proteins.

Protein Digestion

Proteins bound to protein A beads in 50 μL of 10 mM NH_4HCO_3 were incubated with 100 ng of trypsin (sequencing grade; Boehringer Mannheim). After overnight incubation with gentle shaking at room temperature, the pH was decreased to 2 by adding trifluoroacetic acid (TFA) in water up to 0.4% (v/v).

LC/MALDI-TOF/MS Analysis

Fifty microliters of peptide sample was injected into a 100 × 0.25-mm Prontosil 3-μm C18H column (prepared in-house) and eluted at a flow rate of 4 μL/min with 5% (v/v) acetonitrile in water containing 0.05% TFA. A gradient from 5 to 20% (v/v) acetonitrile in water containing 0.05% (v/v) TFA was applied in 90 s, followed by a slower linear increase to 40% (v/v) acetonitrile in water containing 0.05% (v/v) TFA in another 4 min (Alliance 2690 running at 0.25 mL/min equipped with a flow splitter; Waters). Samples were collected directly onto a sample plate (MTP AnchorChip 200/384; Bruker Daltonics) in fractions of 15 s, taking into account the system gradient delay time and column volume before starting collection. After air-drying, 1 μL of a 20× diluted α-cyano-4-hydroxy-cinnamic acid solution was added to each spot. This solution was prepared by diluting a saturated α-cyano-4-hydroxy-cinnamic acid solution (prepared in 50% [v/v] acetonitrile, 49% [v/v] water, and 1% [v/v] TFA) 20 times into the same solution. Sample spots were recrystallized by applying 1.5 μL of 60% (v/v) ethanol, 30% (v/v) acetone, 10% (v/v) water, and 0.1% (v/v) TFA to all samples and allowing them to air-dry.

Mass spectra were measured with a Bruker Ultraflex MALDI-TOF/MS apparatus equipped with a reflectron (Bruker Daltonics) in positive mode with a high precision method. Spectra were measured after external quadratic calibration with a peptide standard mixture containing nine peptides in the mass range between 757 and 3146 D (Bruker Daltonics). In general, spectra were summed for ~500 to 1000 laser pulses (20 Hz; nitrogen laser at 337 nm) and internally recalibrated with protein A–derived peptides and/or trypsin autolysis peaks when present. All *m/z* values also present in the control peptide sample were subsequently removed from the *m/z* list obtained for the immunoprecipitated SERK1 protein complex. Remaining *m/z* values were checked for sodium and/or potassium adducts (differences of 22.990 and 38.946 D, respectively). When found, these *m/z* values were deleted as well. For identification of SERK1, the program GPMAW (http://welcome.to/gpmaw/) was used to determine which *m/z* values corresponded to tryptic peptides from the predicted protein sequence of SERK1. These selected *m/z* values were used as inputs for the MASCOT program to search either the *Arabidopsis* database or all entries without selecting a taxonomy. The posttranslational

modifications phosphorylation (of Ser, Thr, and Tyr) and oxidation of Met were allowed, and a peptide *m/z* tolerance of 100 ppm was used. After identification, the *m/z* values that matched the SERK1 protein were removed from the list before searching for other proteins. Alternatively, the searches were performed with the complete *m/z* list directly using the MASCOT search engine (http://www.matrixscience.com) (Perkins et al., 1999).

Accession Numbers

Sequence data and seed stocks from this article can be found in the GenBank/EMBL data libraries under the following accession numbers: *SERK1* cDNA clone (A67827, At1g71830), *SERK3/BAK1* cDNA clone (AF384970, At4g33430), and *BRI1* cDNA clone (AF017056, At4g39400). The *serk1-1* and *serk3* insertion lines were obtained from the SIGnAL TDNA-Express collection, with accession numbers SALK_544330 and SALK_034523.56.00, respectively. The *serk2-2* insertion line was obtained from the Syngenta *Arabidopsis* insertion lines, with accession number 119-G03. The *bri1-119* and *bri1-4* mutants were obtained from the ABRC, with stock numbers CS399 and 3953, respectively.

Supplemental Data

The following materials are available in the online version of this article.

Supplemental Table 1. *m/z* Values of the Peptides Obtained after Immunoprecipitation of a Total Protein Extract from 10-d-Old Transgenic Seedlings Expressing the SERK1-CFP Fusion Protein.

Supplemental Table 2. Numeric Representation of the Inflorescence Length and Rosette Width of *bri1-119* Mutant Plants and *bri1-119 serk1-1*, *bri1-119 serk2-2*, and *bri1-119 serk3* Double Mutants.

ACKNOWLEDGMENTS

We thank Jan-Willem Borst (Center for Microspectroscopy, Wageningen University) for help with the FLIM, Boudewijn van Veen (Center for Microspectroscopy) for help in editing and formatting the images shown here, and the Nottingham Arabidopsis Stock Centre for supplying the Salk insertion seed lines. We thank Jianming Li (Department of Molecular, Cellular, and Developmental Biology, University of Michigan) for kindly providing the BAK1-GFP transgenic plants. This work was cofinanced by the Center for BioSystems Genomics, which is part of the Netherlands Genomics Initiative/Netherlands Organization for Scientific Research (NWO), by Grant ALW 812.06.004 from the Dutch Organization for Research, NWO (J.A.), and by the Agrotechnology and Food Sciences Group of Wageningen University (E.R., J.V., S.B., and S.d.V.).

Received November 10, 2005; revised January 4, 2006; accepted January 16, 2006; published February 10, 2006.

REFERENCES

Albrecht, C., Russinova, E., Hecht, V., Baaijens, E., and de Vries, S.C. (2005). The *Arabidopsis thaliana* somatic embryogenesis receptor-like kinases 1 and 2 control male sporogenesis. Plant Cell **17,** 3337–3349.

Alonso, J.M., et al. (2003). Genome-wide insertional mutagenesis of *Arabidopsis thaliana.* Science **301,** 653–657.

Becraft, P.W. (2002). Receptor kinase signaling in plant development. Annu. Rev. Cell Dev. Biol. **18,** 163–192.

Colcombet, J., Boisson-Dernier, A., Ros-Palau, R., Vera, C.E., and Schroeder, J. (2005). *Arabidopsis thaliana* somatic embryogenesis receptor kinases 1 and 2 are essential for tapetum development and microspore maturation. Plant Cell **17,** 3350–3361.

Drewes, G., and Bouwmeester, T. (2003). Global approaches to protein-protein interactions. Curr. Opin. Cell Biol. **15,** 199–205.

Feng, X.H., and Derynck, R. (1997). A kinase subdomain of transforming growth factor-beta (TGF-beta) type I receptor determines the TGF-beta intracellular signaling specificity. EMBO J. **16,** 3912–3923.

Friedrichsen, D.M., Joazeiro, C.A., Li, J., Hunter, T., and Chory, J. (2000). Brassinosteroid-insensitive-1 is a ubiquitously expressed leucine-rich repeat receptor serine/threonine kinase. Plant Physiol. **123,** 1247–1256.

Fujita, H., Takemura, M., Tani, E., Nemoto, K., Yokota, A., and Kohchi, T. (2003). An Arabidopsis MADS-box protein, AGL24, is specifically bound to and phosphorylated by meristematic receptor-like kinase (MRLK). Plant Cell Physiol. **44,** 735–742.

Gomez-Gomez, L., Bauer, Z., and Boller, T. (2001). Both the extracellular leucine-rich repeat domain and the kinase activity of FSL2 are required for flagellin binding and signaling in Arabidopsis. Plant Cell **13,** 1155–1163.

Griffiths, S., Dunford, R.P., Coupland, G., and Laurie, D.A. (2003). The evolution of CONSTANS-like gene families in barley, rice, and Arabidopsis. Plant Physiol. **131,** 1855–1867.

Harding, E.W., Tang, W., Nichols, K.W., Fernandez, D.E., and Perry, S.E. (2003). Expression and maintenance of embryogenic potential is enhanced through constitutive expression of AGAMOUS-Like 15. Plant Physiol. **133,** 653–663.

Hecht, V., Vielle-Calzada, J.P., Hartog, M.V., Schmidt, E.D., Boutilier, K., Grossniklaus, U., and de Vries, S.C. (2001). The Arabidopsis SOMATIC EMBRYOGENESIS RECEPTOR KINASE 1 gene is expressed in developing ovules and embryos and enhances embryogenic competence in culture. Plant Physiol. **127,** 803–816.

Heck, G.R., Perry, S.E., Nichols, K.W., and Fernandez, D.E. (1995). AGL15, a MADS domain protein expressed in developing embryos. Plant Cell **7,** 1271–1282.

Kwaaitaal, M.A.C.J., de Vries, S.C., and Russinova, E. (2005). The Arabidopsis somatic embryogenesis receptor kinase 1 protein is present in sporophytic and gametophytic cells and undergoes endocytosis. Protoplasma **226,** 55–65.

Laemmli, U.K. (1970). Cleavage of structural proteins during the assembly of the head of bacteriophage T4. Nature **227,** 680–685.

Li, J., and Chory, J. (1997). A putative leucine-rich repeat receptor kinase involved in brassinosteroid signal transduction. Cell **90,** 929–938.

Li, J., and Nam, K.H. (2002). Regulation of brassinosteroid signaling by a GSK3/SHAGGY-like kinase. Science **295,** 1299–1310.

Li, J., Wen, J., Lease, K.A., Doke, J.T., Tax, F.E., and Walker, J.C. (2002). BAK1, an Arabidopsis LRR receptor-like protein kinase, interacts with BRI1 and modulates brassinosteroid signaling. Cell **110,** 213–222.

Lu, G., DeLisle, A.J., de Vetten, N.C., and Ferl, R.J. (1992). Brain proteins in plants: An Arabidopsis homolog to neurotransmitter pathway activators is part of a DNA binding complex. Proc. Natl. Acad. Sci. USA **89,** 11490–11494.

Mora-Garcia, S., Vert, G., Yin, Y., Cano-Delgado, A., Cheong, H., and Chory, J. (2004). Nuclear protein phosphatases with Kelch-repeat domains modulate the response to brassinosteroids in Arabidopsis. Genes Dev. **18,** 448–460.

Muller, J., Piffanelli, P., Devoto, A., Miklis, M., Elliott, C., Ortmann, B., Schulze-Lefert, P., and Panstruga, R. (2005). Conserved ERAD-like quality control of a plant polytopic membrane protein. Plant Cell **17,** 149–163.

Muslin, A.J., and Xing, H. (2000). 14-3-3 proteins: Regulation of

subcellular localization by molecular interference. Cell. Signal. **12,** 703–709.

Nam, K.H., and Li, J. (2002). BRI1/BAK1, a receptor kinase pair mediating brassinosteroid signaling. Cell **110,** 203–212.

Noguchi, T., Fujioka, S., Choe, S., Takatsuto, S., Yoshida, S., Yuan, H., Feldmann, K.A., and Tax, F.E. (1999). Brassinosteroid-insensitive dwarf mutants of Arabidopsis accumulate brassinosteroids. Plant Physiol. **121,** 743–752.

Pan, S., Sehnke, P.C., Ferl, R.J., and Gurley, W.B. (1999). Specific interactions with TBP and TFIIB in vitro suggest that 14-3-3 proteins may participate in the regulation of transcription when part of a DNA binding complex. Plant Cell **11,** 1591–1602.

Pandey, A., Podtelejnikov, A.V., Blagoev, B., Bustelo, X.R., Mann, M., and Lodish, H.F. (2000). Analysis of receptor signaling pathways by mass spectrometry: Identification of vav-2 as a substrate of the epidermal and platelet-derived growth factor receptors. Proc. Natl. Acad. Sci. USA **97,** 179–184.

Paul, A.L., Sehnke, P.C., and Ferl, R.J. (2005). Isoform-specific subcellular localization among 14-3-3 proteins in Arabidopsis seems to be driven by client interactions. Mol. Biol. Cell **16,** 1735–1743.

Perkins, D.N., Pappin, D.J., Creasy, D.M., and Cottrell, J.S. (1999). Probability-based protein identification by searching sequence databases using mass spectrometry data. Electrophoresis **20,** 3551–3567.

Perry, S.E., Nichols, K.W., and Fernandez, D.E. (1996). The MADS domain protein AGL15 localizes to the nucleus during early stages of seed development. Plant Cell **8,** 1977–1989.

Rancour, D.M., Dickey, C.E., Park, S., and Bednarek, S.Y. (2002). Characterization of AtCDC48. Evidence for multiple membrane fusion mechanisms at the plane of cell division in plants. Plant Physiol. **130,** 1241–1253.

Rancour, D.M., Park, S., Knight, S.D., and Bednarek, S.Y. (2004). Plant UBX domain-containing protein 1, PUX1, regulates the oligomeric structure and activity of Arabidopsis CDC48. J. Biol. Chem. **279,** 54264–54274.

Rienties, I.M., Vink, J., Borst, J.W., Russinova, E., and de Vries, S.C. (2005). The Arabidopsis SERK1 protein interacts with the AAA-ATPase AtCDC48, the 14-3-3 protein GF14lambda and the PP2C phosphatase KAPP. Planta **221,** 394–405.

Rivas, S., Romeis, T., and Jones, J.D. (2002). The Cf-9 disease resistance protein is present in an approximately 420-kilodalton heteromultimeric membrane-associated complex at one molecule per complex. Plant Cell **14,** 689–702.

Rohila, J.S., Chen, M., Cerny, R., and Fromm, M.E. (2004). Improved tandem affinity purification tag and methods for isolation of protein heterocomplexes from plants. Plant J. **38,** 172–181.

Rubio, V., Shen, Y., Saijo, Y., Liu, Y., Gusmaroli, G., Dinesh-Kumar, S.P., and Deng, X.W. (2005). An alternative tandem affinity purification strategy applied to Arabidopsis protein complex isolation. Plant J. **41,** 767–778.

Russinova, E., Borst, J.W., Kwaaitaal, M., Cano-Delgado, A., Yin, Y., Chory, J., and de Vries, S.C. (2004). Heterodimerization and endocytosis of Arabidopsis brassinosteroid receptors BRI1 and AtSERK3 (BAK1). Plant Cell **16,** 3216–3229.

Schagger, H., and von Jagow, G. (1991). Blue native electrophoresis for isolation of membrane protein complexes in enzymatically active form. Anal. Biochem. **199,** 223–231.

Shah, K., Gadella, T.W., Jr., van Erp, H., Hecht, V., and de Vries, S.C. (2001a). Subcellular localization and oligomerization of the *Arabidopsis thaliana* somatic embryogenesis receptor kinase 1 protein. J. Mol. Biol. **309,** 641–655.

Shah, K., Russinova, E., Gadella, T.W., Jr., Willemse, J., and De Vries, S.C. (2002). The Arabidopsis kinase-associated protein phosphatase controls internalization of the somatic embryogenesis receptor kinase 1. Genes Dev. **16,** 1707–1720.

Shah, K., Vervoort, J., and de Vries, S.C. (2001b). Role of threonines in the *Arabidopsis thaliana* somatic embryogenesis receptor kinase 1 activation loop in phosphorylation. J. Biol. Chem. **276,** 41263–41269.

Stone, J.M., Trotochaud, A.E., Walker, J.C., and Clark, S.E. (1998). Control of meristem development by CLAVATA1 receptor kinase and kinase-associated protein phosphatase interactions. Plant Physiol. **117,** 1217–1225.

Torii, K.U. (2004). Leucine-rich repeat receptor kinases in plants: Structure, function, and signal transduction pathways. Int. Rev. Cytol. **234,** 1–46.

Trotochaud, A.E., Hao, T., Wu, G., Yang, Z., and Clark, S.E. (1999). The CLAVATA1 receptor-like kinase requires CLAVATA3 for its assembly into a signaling complex that includes KAPP and a Rho-related protein. Plant Cell **11,** 393–406.

Valverde, F., Mouradov, A., Soppe, W., Ravenscroft, D., Samach, A., and Coupland, G. (2004). Photoreceptor regulation of CONSTANS protein in photoperiodic flowering. Science **303,** 1003–1006.

Wang, H., Tang, W., Zhu, C., and Perry, S.E. (2002a). A chromatin immunoprecipitation (ChIP) approach to isolate genes regulated by AGL15, a MADS domain protein that preferentially accumulates in embryos. Plant J. **32,** 831–843.

Wang, X., Goshe, M.B., Soderblom, E.J., Phinney, B.S., Kuchar, J.A., Li, J., Asami, T., Yoshida, S., Huber, S.C., and Clouse, S.D. (2005a). Identification and functional analysis of in vivo phosphorylation sites of the Arabidopsis BRASSINOSTEROID-INSENSITIVE1 receptor kinase. Plant Cell **17,** 1685–1703.

Wang, X., Li, X., Meisenhelder, J., Hunter, T., Yoshida, S., Asami, T., and Chory, J. (2005b). Autoregulation and homodimerization are involved in the activation of the plant steroid receptor BRI1. Dev. Cell **8,** 855–865.

Wang, Z.Y., Nakano, T., Gendron, J., He, J., Chen, M., Vafeados, D., Yang, Y., Fujioka, S., Yoshida, S., Asami, T., and Chory, J. (2002b). Nuclear-localized BZR1 mediates brassinosteroid-induced growth and feedback suppression of brassinosteroid biosynthesis. Dev. Cell **2,** 505–513.

Williams, R.W., Wilson, J.M., and Meyerowitz, E.M. (1997). A possible role for kinase-associated protein phosphatase in the Arabidopsis CLAVATA1 signaling pathway. Proc. Natl. Acad. Sci. USA **94,** 10467–10472.

Yin, Y., Wang, Z.Y., Mora-Garcia, S., Li, J., Yoshida, S., Asami, T., and Chory, J. (2002). BES1 accumulates in the nucleus in response to brassinosteroids to regulate gene expression and promote stem elongation. Cell **109,** 181–191.

Zhang, S.H., Kobayashi, R., Graves, P.R., Piwnica-Worms, H., and Tonks, N.K. (1997). Serine phosphorylation-dependent association of the band 4.1-related protein-tyrosine phosphatase PTPH1 with 14-3-3beta protein. J. Biol. Chem. **272,** 27281–27287.

Zhang, S.H., Liu, J., Kobayashi, R., and Tonks, N.K. (1999). Identification of the cell cycle regulator VCP (p97/CDC48) as a substrate of the band 4.1-related protein-tyrosine phosphatase PTPH1. J. Biol. Chem. **274,** 17806–17812.